

# A dynamical systems approach for the station keeping of a Solar Sail

Ariadna Farrés and Àngel Jorba  
Departament de Matemàtica Aplicada i Anàlisi  
Universitat de Barcelona  
Gran Via 585, 08007 Barcelona, Spain  
E-mails: [ari@maia.ub.es](mailto:ari@maia.ub.es), [angel@maia.ub.es](mailto:angel@maia.ub.es)

10th December 2007

## **Abstract**

In this paper we have considered the movement of a solar sail in the Sun - Earth system. As a model we have used the RTBP adding the solar radiation pressure. It can be seen that we have a 2D family of equilibria parametrised by the two angles defining the sail orientation. Most of these equilibrium points are unstable and require a control strategy to keep the sail close to them. We have designed a control strategy that uses the knowledge of the position of the invariant manifolds and how they vary when the sail orientation is changed. We have tested our strategy with two known missions: the Polar Observer and the Geostorm Warning Mission. Simulations up to 30 years have been done taking into account errors on the position and velocity determination of the sail and on the sail orientation.

# Contents

<b>1</b>	<b>Introduction</b>	<b>3</b>
<b>2</b>	<b>Equations of Motion</b>	<b>4</b>
<b>3</b>	<b>Equilibrium Points</b>	<b>5</b>
3.1	Linearisation with respect to $\alpha$ and $\delta$ . . . . .	7
<b>4</b>	<b>Station Keeping</b>	<b>7</b>
4.1	Dynamics Near a Fixed Point . . . . .	8
4.1.1	Saddle Behaviour . . . . .	10
4.1.2	Centre Behaviour . . . . .	13
4.2	Choosing the New Sail Orientation $(\alpha, \delta)$ . . . . .	15
4.3	Summary of the Control Algorithm . . . . .	17
<b>5</b>	<b>Mission Application</b>	<b>17</b>
5.1	The Geostorm Mission . . . . .	18
5.1.1	Mission Orbit . . . . .	19
5.2	The Polar Observer Mission . . . . .	20
5.2.1	Mission Orbit . . . . .	23
<b>6</b>	<b>Sensitivity to Errors During the Control Strategy</b>	<b>27</b>
<b>7</b>	<b>Conclusions</b>	<b>30</b>
<b>8</b>	<b>Acknowledgements</b>	<b>30</b>

# 1 Introduction

Solar sailing is a proposed form of spacecraft propulsion using large membrane mirrors. The impact of the photons emitted by the Sun on the surface of the sail and their further reflection produce momentum on it. Although the acceleration produced by this reflection is smaller than the one achieved by a 'traditional' spacecraft it is continuous and illimited. This makes some long term missions more accessible.

A solar sail is an orientable surface, the orientation of the sail is defined by two angles, the pitch ( $\alpha$ ) and yaw ( $\delta$ ) angle. Another important parameter is the Sail lightness number ( $\beta$ ) used to define the sail effectiveness [9]. In this paper we have considered that the sail is a perfectly reflecting surface, so the force due to the solar radiation pressure is normal to the surface of the sail.

To model the dynamics of the solar sail we have considered that Earth and Sun are point masses moving in a circular way around their common centre of masses. The sail is then affected by the gravitational attraction of Earth and Sun and by the solar radiation pressure. We have taken a synodical transformation so that Sun and Earth are fixed on the  $x$ -axis. As we will see this system is a perturbation of the Restricted Three Body Problem (RTBP).

It is well know that the RTBP has five equilibrium points ( $L_{1,\dots,5}$ ). For a small  $\beta$  these five equilibrium points are replaced by five continuous families of equilibria parametrised by the sail orientation ( $\alpha, \delta$ ). As  $\beta$  increases 4 of these families merge and the fixed points form two connected surfaces  $S_1$  and  $S_2$ . In [9] it can be seen that  $S_1$  is diffeomorphic to a sphere and  $S_2$  is diffeomorphic to a torus.

The stability of these fixed points will also be discussed. As it is also mentioned in [9] most of the fixed points are unstable. If we focus on the eigenvalues of the linearisation we can classify the fixed points in three classes. One class that contains those fixed points with three pairs of complex eigenvalues, a second class with the fixed points with one pair of real eigenvalues and two pairs of complex eigenvalues and a third class with fixed points with 2 pair of real eigenvalues and one pair of complex eigenvalues. From now on we will focus on the points of the second class. Although the complex eigenvalues can have real positive part this one will be very small compared with the instability produced by the real eigenvalues. Hence, as a first approximation we will start assuming that the linear dynamics around these fixed points is saddle  $\times$  centre  $\times$  centre. The real effect will be taken into account later on.

If the sail orientation is changed, the equilibrium point  $p_0$  will vary and so will the eigenvalues and eigendirections. We want to understand the linear dynamic around the equilibrium point and how it varies with the sail orientation to be able to design a control strategy to keep a probe close to a fixed point.

When the probe is close to the fixed point  $p_0$ , the trajectory escapes along the unstable direction. We want to change the sail orientation  $\alpha = \alpha_1, \delta = \delta_1$  so that the unstable direction of the new equilibrium point brings the trajectory close to the stable direction of  $p_0$ . Then we will restore the original sail orientation and so on. Let us notice that the projection of the trajectory on the central behaviour are rotations around the different equilibrium points. This process might produce an unbounded trajectory, so we have to

take into account the central behaviour when choosing the new sail orientation.

In the literature ([9], [12], [1]) we can find two different missions that need to keep a solar sail close to an unstable fixed point. These two missions are the Geostorm Warning Enhanced and the Polar Observer. In sections 5.1 and 5.2 we give a small overview of the main objectives of these two missions and we have applied our control strategy to them. 1000 simulations with random initial conditions has been done and the results are successful. As we will see for all of these initial conditions the control strategy manages to keep the sail close to the equilibrium point.

We have also tested our control strategy with different fonts of errors. We have introduced errors on the sail orientation and errors in the position determination. The errors on the sail orientation will affect to the probe's trajectory and the second type of errors will affect to the decisions taken by the control strategy. We have made 1000 simulations with the same initial conditions as before including these two effects. We will discuss the effect of these errors in both missions. A summarised version of the results can be found in [3] and [2].

## 2 Equations of Motion

We assume that Earth and Sun are point masses moving in circular orbits around their common centre of mass. The units of mass, distance and time are normalised so that the total mass of the system is 1, the Earth-Sun distance is 1 and the period of the orbits is  $2\pi$ . With these units, the gravitational constant is also 1. We focus on the motion of a probe under the gravitational attraction of these two bodies and the effect of the solar radiation pressure. We use a rotating reference system so that Earth and Sun are fixed on the  $x$  axis,  $z$  is perpendicular to the ecliptic plane and  $y$  defines a orthogonal positive oriented reference system (Figure 1, left).

The force of the solar radiation pressure depends on the position of the probe, the orientation and the characteristic acceleration of the sail. The orientation of the sail is defined by two angles, say  $\alpha$  and  $\delta$ :  $\alpha$  is the angle between the Sun-line and the projection on the ecliptic plane of the normal vector to the sail  $\vec{n}$ ;  $\delta$  is the angle between the ecliptic plane and  $\vec{n}$  (see Figure 1, right). As the vector  $\vec{n}$  cannot point towards the Sun then  $\alpha \in [-\pi/2, \pi/2]$  and  $\delta \in [-\pi/2, \pi/2]$ . There are other possibilities to define these angles, see [9], [6], [10]. The equations of motion for the probe are

$$\begin{aligned}\ddot{x} &= 2\dot{y} + x - (1 - \mu)\frac{x - \mu}{r_{PS}^3} - \mu\frac{x + 1 - \mu}{r_{PT}^3} + \kappa \cos(\phi(x, y) + \alpha) \cos(\psi(x, y, z) + \delta), \\ \ddot{y} &= -2\dot{x} + y - \left(\frac{1 - \mu}{r_{PS}^3} + \frac{\mu}{r_{PT}^3}\right) y + \kappa \sin(\phi(x, y) + \alpha) \cos(\psi(x, y, z) + \delta), \\ \ddot{z} &= -\left(\frac{1 - \mu}{r_{PS}^3} + \frac{\mu}{r_{PT}^3}\right) z + \kappa \sin(\psi(x, y, z) + \delta),\end{aligned}\tag{1}$$

where  $\kappa = \beta \frac{1 - \mu}{r_{PS}^2} \cos^2 \alpha \cos^2 \delta$ ,  $\beta$  is the sail lightness number (it measures the effectiveness

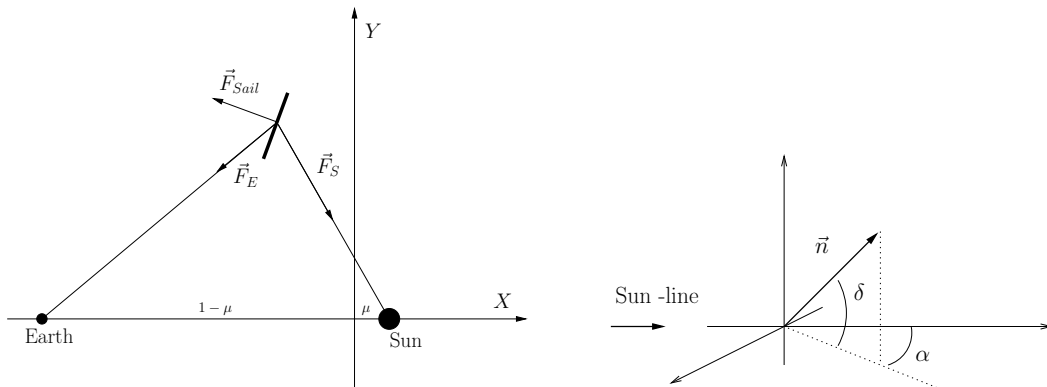


Figure 1: *Left: Forces due to the sail and the gravitational attraction of the Earth and Sun. Right: Relation between the sail angles ( $\alpha$  and  $\delta$ ) and the Sun-line,  $\vec{n}$  is the normal direction to the surface of the sail.*

of the sail), and the angles  $\phi(x, y)$ ,  $\psi(x, y, z)$  refer to the position of the probe w.r.t. the Sun:

$$\phi(x, y) = \arctan\left(\frac{y}{x - \mu}\right), \quad \psi(x, y, z) = \arctan\left(\frac{z}{\sqrt{(x - \mu)^2 + y^2}}\right), \quad (2)$$

with  $\phi(x, y) \in [-\pi, \pi]$  and  $\psi(x, y, z) \in [-\pi/2, \pi/2]$ . Note that the equations of motion depend on three parameters:  $\beta$ ,  $\alpha$  and  $\delta$ . It is clear that if  $\beta = 0$  (i.e. no sail) or  $\alpha = \pm\pi/2$  or  $\delta = \pm\pi/2$  (i.e. sail aligned with the Sun-line, so no sail effect) the equations are the same as in the Restricted Three Body Problem (RTBP).

### 3 Equilibrium Points

For a good understanding of the dynamics of the system we need to know the invariant objects. First of all we will compute the fixed points for different sail orientations.

The equations for the fixed points are obtained by setting  $\dot{x} = \ddot{x} = \dot{y} = \ddot{y} = \dot{z} = \ddot{z} = 0$  in (1). As we have already mentioned, for  $\alpha = \pm\pi/2$  or  $\delta = \pm\pi/2$  this model coincides with the RTBP, hence, it has five well known equilibrium points  $L_{1,\dots,5}$  (see [11]). It is easy to see that for small  $\beta$ , these points are replaced by five continuous families of equilibria parametrised by  $\alpha, \delta$ .

If  $\alpha = \delta = 0$  (i.e. the sail is normal to the Sun-line), there are three new equilibria on the Earth-Sun line, known as Sub- $L_{1,2,3}$  equilibrium points. These new points can be obtained by solving (numerically) a suitable quintic equation. Sub- $L_1$  and Sub- $L_3$  are closer to the Sun than  $L_1$  and  $L_3$  and Sub- $L_2$  is between  $L_2$  and the Earth as can be seen in Figure 2. These points depend on the sail lightness number ( $\beta$ ), as  $\beta$  increases all Sub- $L_i$  come closer to the Sun.

The equilibrium points are organised in 2-D families parametrised by  $\alpha$  and  $\delta$ . We have computed these families numerically by means of a continuation method. For small

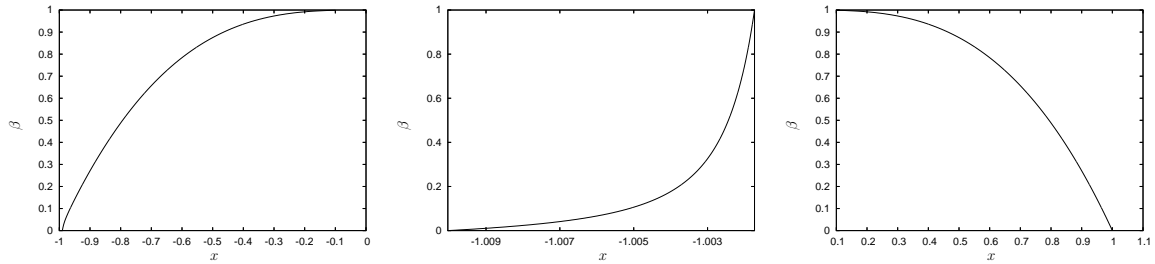


Figure 2: Relation between the fixed points ( $Sub-L_i$ ) and  $\beta$ . On the vertical axis we have the different values of  $\beta$  and on the horizontal axis the  $x$  coordinate of the fixed point. From left to right  $Sub-L_1$ ,  $Sub-L_2$  and  $Sub-L_3$

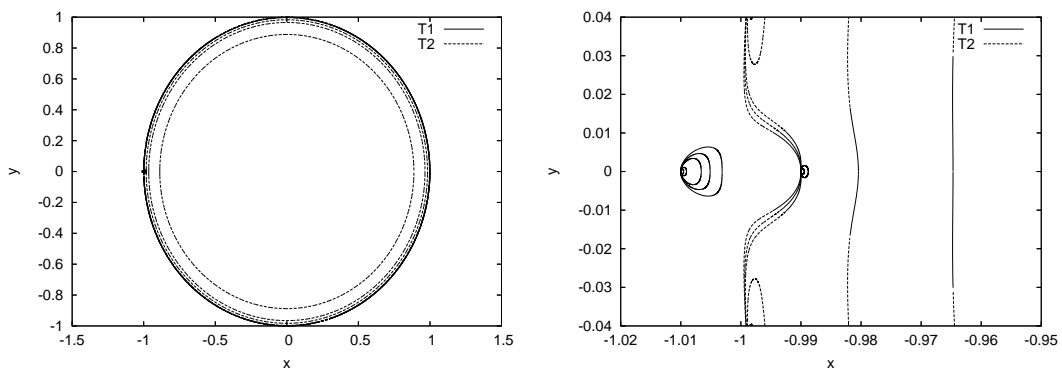


Figure 3: Equilibrium points in the  $\{x, y\}$ - plane for  $\beta_1 = 0.005, \beta_2 = 0.01, \beta_3 = 0.05, \beta_4 = 0.1, \beta_5 = 0.3$ . The  $T_1$  points have a pair of real eigenvalues and two pair of complex eigenvalues and the  $T_2$  points have three complex eigenvalues.

values of  $\beta$  the fixed points are in five continuous families of equilibria. As  $\beta$  increases 4 of these families merge and the fixed points are on two disconnected surfaces,  $S_1$  and  $S_2$ .  $S_1$  contains the points  $L_2$  and  $Sub-L_2$  and  $S_2$  contains  $L_{1,3,4,5}$  and  $Sub-L_{1,3}$ . It can be seen that for a fixed  $\beta$   $S_1$  is diffeomorphic to a sphere, and it is situated on the vicinity of  $L_2$ . On the other hand,  $S_2$  is diffeomorphic to a torus and is located around the Sun.

In Figure 3 we can see a slice of these surfaces for  $z = 0$  for different values of  $\beta$  and Figure 4 shows the slice for  $y = 0$  for different values of  $\beta$ . All these points are unstable,  $T_1$  are those fixed points with one pair of real eigenvalue and two pairs of complex eigenvalues,  $T_2$  are those with three pair of complex eigenvalues and  $T_3$  those with two pairs of real eigenvalues and a pair of complex eigenvalues.

It is well known ([11]) that the  $L_{1,2,3}$  are unstable points, with a pair of real eigenvalues and two pairs of complex eigenvalues with zero real part and that  $L_{4,5}$  in the Earth-Sun system are linearly stable with three pairs of complex eigenvalues with zero real part. When the sail lightness number  $\beta$  is different from zero, the  $Sub-L_{1,2,3}$  points branch off from the classical  $L_{1,2,3}$  points and it can be seen that they are also unstable with a pair of real eigenvalues and two pairs of complex eigenvalues with zero real part.

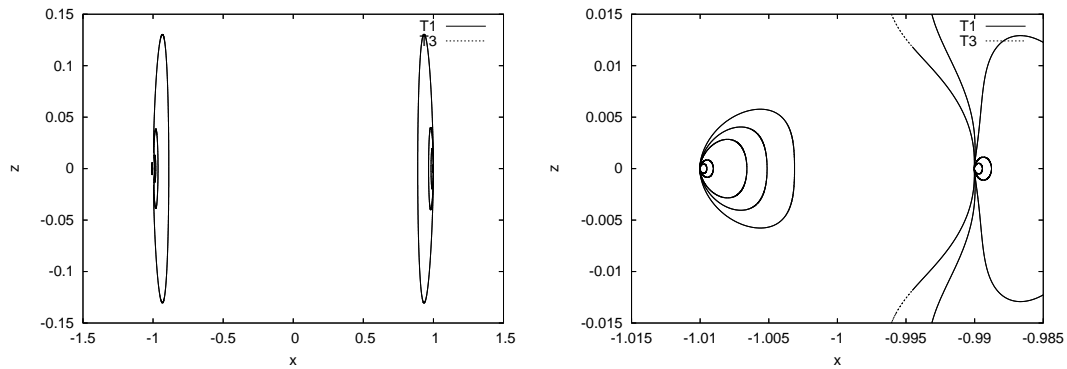


Figure 4: *Equilibrium points in the  $\{x, z\}$  plane for  $\beta_1 = 0.005, \beta_2 = 0.01, \beta_3 = 0.05, \beta_4 = 0.1, \beta_5 = 0.3$ . The  $T_1$  points have a pair of real eigenvalues and two pair of complex eigenvalues and the  $T_3$  points have two pair of real eigenvalues and one pair of complex eigenvalues.*

In [9] McInnes shows that the equilibrium points of this system are in general unstable. We can see that close to  $L_{1,2,3}$  and  $\text{Sub-}L_{1,2,3}$  these points have a pair of real eigenvalues and two pair of complex eigenvalues. In this work we will focus on these type of equilibrium points.

### 3.1 Linearisation with respect to $\alpha$ and $\delta$

From now on, the value of lightness of the sail,  $\beta$ , will be considered fixed. We are interested in knowing the variation of the fixed points when we change  $\alpha$  and  $\delta$ .

If  $p_0 = p(\alpha_0, \delta_0)$  are the coordinates of a fixed point of  $\dot{X} = f(X, \alpha, \delta)$  then  $f(p_0, \alpha_0, \delta_0) = 0$ . The Implicit Function Theorem implies that  $\frac{\partial p}{\partial \alpha}(\alpha_0, \delta_0)$  and  $\frac{\partial p}{\partial \delta}(\alpha_0, \delta_0)$  are found by solving,

$$\begin{aligned} D_X f(p_0, \alpha_0, \delta_0) \frac{\partial p}{\partial \alpha}(\alpha_0, \delta_0) &= -\frac{\partial f}{\partial \alpha}(p_0, \alpha_0, \delta_0), \\ D_X f(p_0, \alpha_0, \delta_0) \frac{\partial p}{\partial \delta}(\alpha_0, \delta_0) &= -\frac{\partial f}{\partial \delta}(p_0, \alpha_0, \delta_0). \end{aligned}$$

As we do not know explicitly  $p(\alpha, \delta)$  and the angles will only be moved in a small amount, we will deal with the linear approximation. Close to  $p(\alpha_0, \delta_0)$ :

$$p(\alpha, \delta) = p(\alpha_0, \delta_0) + Dp \cdot h, \quad (3)$$

where  $h = (\alpha - \alpha_0, \delta - \delta_0)^T$  and  $Dp = \left( \frac{\partial p}{\partial \alpha}(\alpha_0, \delta_0), \frac{\partial p}{\partial \delta}(\alpha_0, \delta_0) \right)$ .

## 4 Station Keeping

In this section we will focus on a linearly unstable equilibrium point and we will use the information on its local dynamics to design a control strategy. The use of solar radiation

pressure and the unstable manifolds to stabilise a satellite on a Halo orbit has been considered before (see [4], reprinted in [5]).

Here the main idea is to change the sail orientation (i.e. the phase space) to make the system act as we wish. When the spacecraft is close enough to a fixed point the linearisation of the equations of motion around the equilibrium point gives an accurate description of the dynamics. In Section 3 we have mentioned that most of the unstable points have two real eigenvalues ( $\pm\lambda$ ) and two pairs of complex eigenvalues. One of the pairs of complex eigenvalues can have non-zero real part ( $\nu_1 \pm i\omega_1$ ) and the other pair of eigenvalues is purely imaginary ( $\pm i\omega_2$ ).

From now on we will make the assumption that  $\nu_1 = 0$ , supposing that the dynamics given in this central direction is a rotation around the origin instead of spiralling inwards or outwards, depending on the sign of  $\nu_1$ . If  $\nu_1 < 0$  our supposition just adds more difficulties on the central behaviour as this is naturally stable. Instead, if  $\nu_1 > 0$  the trajectories will spiral outwards and our control strategy can fail. We will see that the control strategy can minimise the central behaviour. If this minimisation is bigger than the expansion that the spiral experiences we will be able to control the sail. Also, as  $\nu_1 \approx 0$  this spiralling is really small and it is not very relevant for short times. Hence, here we assume that the linear dynamics around the fixed points is saddle  $\times$  centre  $\times$  centre.

Let  $p_0$  be the fixed point for  $\alpha = \alpha_0$  and  $\delta = \delta_0$ . If the sail is close to  $p_0$  its trajectory will escape along the unstable direction. We want to change the orientation of the sail ( $\alpha = \alpha_1, \delta = \delta_1$ ) so that the unstable direction of this new fixed point sends the probe back to the neighbourhood of  $p_0$ . Then, we restore the initial orientation of the sail,  $\alpha = \alpha_0$  and  $\delta = \delta_0$ , and so on. This is graphically shown in Figure 5. It is important to note that, during this process, the projection of the dynamics into the central part of the equilibria can grow: as the central behaviour are rotations around each of the fixed points, the composition of central motions with different centre of rotation can result in an unbounded growth of the central component of the motion. For this reason we have to be careful when we chose the sail orientation. We have to control the instability given by the unstable direction and to make sure that the central behaviour does not grow.

## 4.1 Dynamics Near a Fixed Point

As it has been said previously we are supposing that the linear behaviour close to the fixed points is saddle  $\times$  centre  $\times$  centre. Let  $p_0 \in \mathbb{R}^6$  be the fixed point and  $\pm\lambda$ ,  $\pm i\omega_1$  and  $\pm i\omega_2$  the eigenvalues. If the sail orientation is slightly changed then  $p_0$  is also slightly changed as well as the eigenvalues and eigenvectors.

From now on we will describe the trajectory of the probe by its projection on the three different planes centred on  $p_0$ . The first one is generated by the two eigenvector with real eigenvalues ( $\vec{v}_1, \vec{v}_2$ ), where the saddle behaviour is described. The other two are generated by the real and imaginary part of the two pairs of complex eigenvectors ( $\vec{v}_i, \vec{v}_{i+1}$  for  $i = 3, 5$ ). The projection of the orbit on these two planes describes the central behaviour of the motion. In this reference system the trajectory of the probe is given by  $(x_1(t), y_1(t), x_2(t), y_2(t), x_3(t), y_3(t))$  (see Figure 6).

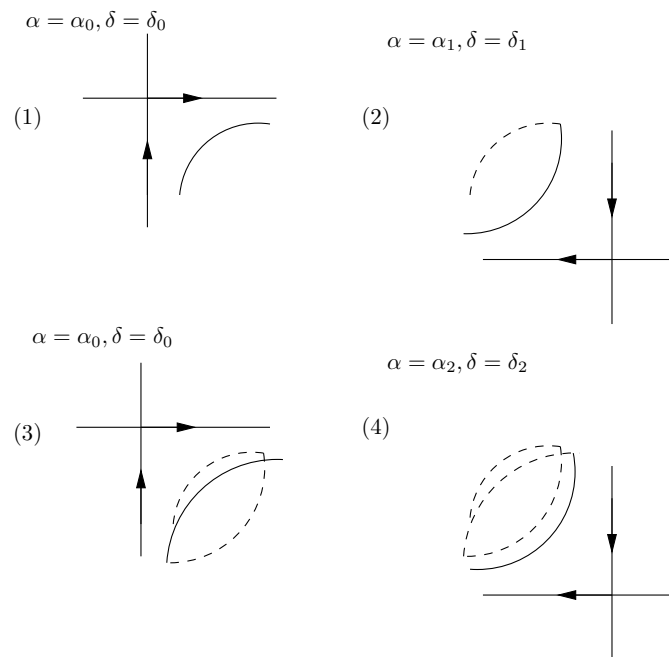


Figure 5: *Idea of how to control the saddle behaviour.*

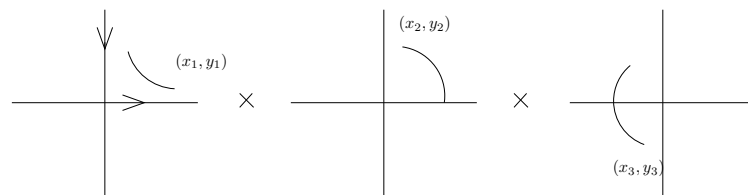


Figure 6: *Schematic representation of the trajectory of the sail in the  $\{p_0; \vec{v}_1, \dots, \vec{v}_6\}$  reference system*

We want to obtain a sail orientation so that the unstable direction of the new fixed point brings the probe back to a neighbourhood close to the initial fixed point  $p_0$ . As we know the fixed points live in a 2D surface and we have a 6D phase space, so we have some limitations in the positions of the new fixed point.

In sections 4.1.1 and 4.1.2 we will describe the saddle and centre behaviour of the trajectory and will show where the fixed point should be placed to deal with the instability. We will first suppose that we have free choice in the fixed points position, and then in Section 4.2 we will see how to chose the sail orientation, taking into account the limitations on the fixed points position.

#### 4.1.1 Saddle Behaviour

Suppose that for  $\alpha = \alpha_0$  and  $\delta = \delta_0$  the fixed point is at the origin so the motion of the saddle part is,

$$\left. \begin{aligned} x_1(t) &= x_{10}e^{\lambda(t-t_0)} \\ y_1(t) &= y_{10}e^{-\lambda(t-t_0)} \end{aligned} \right\}, \quad (4)$$

where  $(x_{10}, y_{10})$  is the initial condition.

When the sail orientation is changed  $\alpha = \alpha_0 + \epsilon_\alpha$  and  $\delta = \delta_0 + \epsilon_\delta$  the fixed point and the eigenvalues and eigenvectors change slightly. From now on we will just consider that the eigenvectors are the same as the ones at the origin. If  $(\bar{x}_1, \bar{y}_1)$  is the new fixed point and  $\pm\bar{\lambda}$  are the real eigenvalues for  $(\bar{x}_1, \bar{y}_1)$ , then the movement of the probe is,

$$\left. \begin{aligned} \bar{x}_1(t) &= \bar{x}_1 + (\bar{x}_{10} - \bar{x}_1)e^{\bar{\lambda}(t-t_0)} \\ \bar{y}_1(t) &= \bar{y}_1 + (\bar{y}_{10} - \bar{y}_1)e^{-\bar{\lambda}(t-t_0)} \end{aligned} \right\}, \quad (5)$$

where  $(\bar{x}_{10}, \bar{y}_{10})$  is the initial condition.

To control the saddle behaviour we will define two bounds  $B_1 = \{x_1 = \varepsilon_{min}\}$  (the minimal distance to the stable direction) and  $B_2 = \{x_1 = \varepsilon_{max}\}$  (the maximal distance to the stable direction), that define the region of movement (between  $B_1$  and  $B_2$ ). When the trajectory reaches one of these two bounds the sail orientation is changed. We will determine  $\varepsilon_{min}$  and  $\varepsilon_{max}$  depending on the mission interest and the phase space properties.

If the sail orientation is fixed to  $\alpha = \alpha_0$  and  $\delta = \delta_0$  the trajectory followed is given by (4) and goes from  $B_1$  to  $B_2$ . When the sail orientation is changed to  $\alpha = \alpha_1$  and  $\delta = \delta_1$  the trajectory is given by (5). The initial condition for one movement is the end condition of the other movement. From now on we will refer to the points where we change the sail orientation as change points.

In order to control the instability the new fixed point  $(\bar{x}_1, \bar{y}_1)$  must be chosen so that  $\bar{x}_1 > \varepsilon_{max}$ . As we are supposing that all the eigenvectors are the same then the new fixed points unstable direction will bring the probe back to  $B_1$  (see Figure 7).

Going from  $B_1$  to  $B_2$ , the trajectories follow (4), with  $x_{10} = \varepsilon_{min}$  and  $x_1(t_f) = \varepsilon_{max}$  so  $\varepsilon_{max} = \varepsilon_{min}e^{\lambda\Delta t_1}$  and

$$\Delta t_1 = \frac{1}{\lambda} \log \left( \frac{\varepsilon_{max}}{\varepsilon_{min}} \right). \quad (6)$$

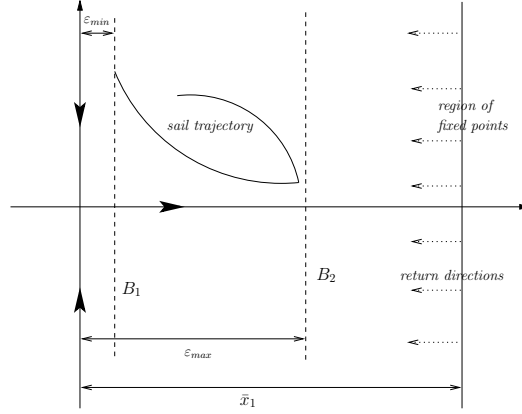


Figure 7: Representation of the important parameters in the control of the saddle part. The bounce region is the location of the future fixed points, we will chose one of them, and the bounce direction are the eigendirections for those fixed points.

Going from  $B_2$  to  $B_1$ , the trajectories follow (5), with  $\bar{x}_{10} = \varepsilon_{max}$  and  $\bar{x}_1(t_f) = \varepsilon_{min}$  so  $\varepsilon_{min} = \bar{x}_1 + (\varepsilon_{max} - \bar{x}_1)e^{\lambda\Delta t_2}$  and

$$\Delta t_2 = \frac{1}{\lambda} \log \left( \frac{\bar{x}_1 - \varepsilon_{min}}{\bar{x}_1 - \varepsilon_{max}} \right). \quad (7)$$

Notice that  $\Delta t_2$  varies with the fixed point as it also depends on  $\bar{\lambda}$ .

Let  $t_i$  for  $i \in \mathbb{N}$  be the instant of time when the probe is at one of the bounds  $B_{1,2}$ . We will suppose that  $t_0 = 0$  and that the probe is initially placed in  $B_1$ . Then,

$$\begin{aligned} t_{2i+1} &= t_{2i} + \Delta t_1, \\ t_{2i+2} &= t_{2i+1} + \Delta t_2, \end{aligned}$$

for  $i \in \mathbb{N}$ , where  $t_{2i}$  i.e. the time when the probe is placed at  $B_1$  and  $t_{2i+1}$  when it is placed at  $B_2$ .

Let  $(\zeta_1^{(i)}, \eta_1^{(i)})$  be the sequence of change points, where for  $i$  even the change points are in  $B_1$  ( $\zeta_1^{(i)} = \varepsilon_{min}$ ) and for  $i$  odd they are in  $B_2$  ( $\zeta_1^{(i)} = \varepsilon_{max}$ ). The following lemma shows how the sequence of new fixed points  $(\bar{x}_1^{(i)}, \bar{y}_1^{(i)})$  has to be taken to control the saddle instability.

**Lemma 4.1** *Let  $(\bar{x}_1^{(i)}, \bar{y}_1^{(i)})$  be the sequence of new fixed points for the control strategy and  $(\zeta_1^{(i)}, \eta_1^{(i)})$  the sequence of change points. If we choose  $\bar{y}_1^{(i)} = \eta_1^{(2i+1)}$  and  $\bar{x}_1^{(i)} = \xi$  with  $\xi > \varepsilon_{max}$ , then*

$$\lim_{i \rightarrow \infty} \bar{y}_1^{(i)} = 0,$$

so the control strategy new fixed points tend to  $(\xi, 0)$  and the saddle behaviour is stabilised.

**Proof**

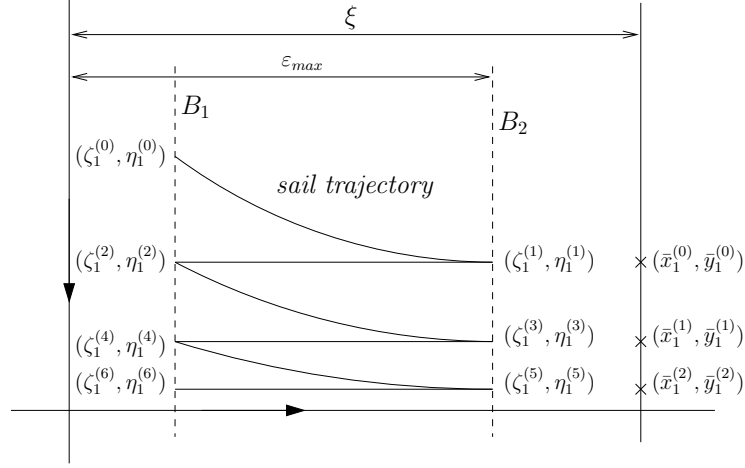


Figure 8: Sequence of fixed points and the projection of the probe's trajectory in the saddle plane.

We will see by induction that  $\eta_1^{(2n+1)} = \eta_1^{(0)} \left( \frac{\varepsilon_{min}}{\varepsilon_{max}} \right)^n$ .

For  $n = 1$ ,

$$\eta_1^{(1)} = y_1(t_0 + \Delta t_1) = \eta_1^{(0)} e^{-\lambda \Delta t_1} = \eta_1^{(0)} \left( \frac{\varepsilon_{min}}{\varepsilon_{max}} \right).$$

We suppose it is true for  $n = i$ , and we will show it holds for  $n = i + 1$ .

$$\eta_1^{(2i+3)} = y_1(t_{2i+2} + \Delta t_1) = \eta_1^{(2i+2)} e^{-\lambda \Delta t_1} = \eta_1^{(2i+2)} \left( \frac{\varepsilon_{min}}{\varepsilon_{max}} \right), \quad (8)$$

where

$$\eta_1^{(2i+2)} = \bar{y}_1(t_{2i+1} + \Delta t_2) = \bar{y}_1^{(i)} + (\eta_1^{(2i+1)} - \bar{y}_1^{(i)}) e^{-\lambda \Delta t_2},$$

as we are considering  $\bar{y}_1^{(i)} = \eta_1^{(2i+1)} \Rightarrow \eta_1^{(2i+2)} = \eta_1^{(2i+1)}$ . Then by the induction hypothesis equation (8) becomes,

$$\eta_1^{(2i+3)} = \eta_1^{(0)} \left( \frac{\varepsilon_{min}}{\varepsilon_{max}} \right)^{i+1}. \quad (9)$$

As  $\varepsilon_{max} > \varepsilon_{min}$ ,

$$\lim_{n \rightarrow \infty} \bar{y}_1^{(n)} = \lim_{n \rightarrow \infty} \eta_1^{(0)} \left( \frac{\varepsilon_{min}}{\varepsilon_{max}} \right)^n = 0.$$

□

Choosing this sequence of new fixed points  $((\bar{x}_1^{(i)}, \bar{y}_1^{(i)}) = (\xi, \eta_1^{(2i+1)})$  with  $\xi > \varepsilon_{max}$ ) we can stabilise the saddle part of the movement (see Figure 8).

Notice that if the new fixed points satisfy the condition in lemma 4.1 but taking  $\bar{y}_1^{(i)}$  close to  $\eta_1^{(2i+1)}$  the saddle behaviour will also be controlled, although the sequence of fixed points may not converge.

### 4.1.2 Centre Behaviour

Suppose that for  $\alpha = \alpha_0$ ,  $\delta = \delta_0$  the fixed point is at the origin and let  $(x_{20}, y_{20})$  be the initial condition. Then if  $r_0 = \sqrt{x_{20}^2 + y_{20}^2}$  and  $\tau_0 = \arctan\left(\frac{y_{20}}{x_{20}}\right)$ ,

$$\left. \begin{aligned} x_2(t) &= r_0 \cos(\omega_1(t - t_0) + \tau_0) \\ y_2(t) &= r_0 \sin(\omega_1(t - t_0) + \tau_0) \end{aligned} \right\}. \quad (10)$$

When the sail orientation is changed to  $\alpha = \alpha_0 + \epsilon_\alpha$  and  $\delta = \delta_0 + \epsilon_\delta$ , the fixed point changes as well as the eigenvalues and eigenvectors. As before we will just consider that the eigenvectors are the same as the ones at the origin. If  $(\bar{x}_2, \bar{y}_2)$  is the new fixed point and  $\pm i\bar{\omega}_1$  are the pair of complex eigenvalues for  $(\bar{x}_2, \bar{y}_2)$ . Then,

$$\left. \begin{aligned} \bar{x}_2(t) &= \bar{x}_2 + \bar{r}_0 \cos(\bar{\omega}_1(t - t_0) + \bar{\tau}_0) \\ \bar{y}_2(t) &= \bar{y}_2 + \bar{r}_0 \sin(\bar{\omega}_1(t - t_0) + \bar{\tau}_0) \end{aligned} \right\}, \quad (11)$$

where  $\bar{r}_0 = \sqrt{(\bar{x}_2 - \bar{x}_{20})^2 + (\bar{y}_2 - \bar{y}_{20})^2}$ ,  $\bar{\tau}_0 = \arctan\left(\frac{\bar{y}_2 - \bar{y}_{20}}{\bar{x}_2 - \bar{x}_{20}}\right)$  and  $(\bar{x}_{20}, \bar{y}_{20})$  is the initial condition.

The control on the saddle part fixes the time between manoeuvres, in Section 4.1.1 we have seen how to estimate  $\Delta t_1$  and  $\Delta t_2$  (remember  $\Delta t_2$  varies with the fixed point). So the movement in the centre part will be a sequence of rotations around each of the fixed points. The rotations around the origin will be of angle  $\theta_1 = \omega_1 \Delta t_1$  and the rotations around the different fixed points will be of  $\theta_2 = \bar{\omega}_1 \Delta t_2$ , where also  $\theta_2$  varies with the fixed point.

The composition of rotations around different fixed points does not need to be bounded. We would like to place the fixed points so that this movement does not grow. In fact we will find a sequence of fixed points so that the trajectory tends to the equilibrium point.

We are assuming that, for  $\alpha = \alpha_0$ ,  $\delta = \delta_0$  the fixed point is at the origin and the trajectory is an arc starting at the initial condition  $(x_{20}, y_{20})$  and radius  $r_0 = \sqrt{x_{20}^2 + y_{20}^2}$ . Let  $(\zeta_2, \eta_2)$  be the change point, we want to find a fixed point  $(\bar{x}_2, \bar{y}_2)$  so that arc described around this fixed point ends closer to the origin than  $(x_{20}, y_{20})$ .

Depending on the position of  $(\bar{x}_2, \bar{y}_2)$  with respect to the  $(\zeta_2, \eta_2)$  the arc will or will not be totally included in the disk centred at the origin and radius  $r_0$  ( $D_0$ ). We are interested in taking fixed point so that the arc described by the probe is totally included in  $D_0$  (see Figure 9).

It is true that knowing the arc of rotation  $\theta_2$  there are lots of fixed points that can describe an arc totally included in  $D_0$ , but as we are not going to know  $\theta_2$  exactly, as it depends on the fixed point, we need to find fixed points so that  $\forall \theta_2 \in [0, 2\pi]$  the arc described is included in  $D_0$ .

**Lemma 4.2** *Let  $D_0$  be the disk centred at the origin and of radius  $r_0 = \sqrt{x_{20}^2 + y_{20}^2}$  and  $(\zeta_2, \nu_2)$  the change point on  $\partial D_0$ . Then all the fixed points  $(\bar{x}_2, \bar{y}_2)$  such that  $\bar{x}_2 = s \cdot \zeta_2$ ,  $\bar{y}_2 = s \cdot \eta_2$  and  $s \in [0, 1)$  describe an arc included in  $D_0 \forall \theta_2 \in [0, 2\pi]$ . If  $s = 1/2$  the distance to the origin of the end point of the arc is minimal.*

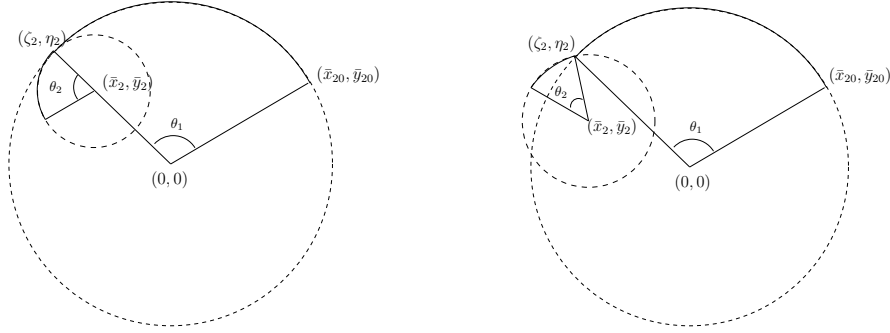


Figure 9: *Left: Relative position of a fixed point so that the arc described by the probe is included in  $D_0$ . Right: Relative position of a fixed point so that the arc describe by the probe is NOT included in  $D_0$*

### Proof

If two disks coincide in one point, one is included in the other if only if these two disks are tangential and the centres are included in the biggest disk. So we are looking for arc's tangential to  $D_0$  and with the centre included in  $D_0$ .

If  $(\zeta_2, \eta_2)$  is the change point and  $(\bar{x}_2, \bar{y}_2)$  is the fixed point, the arc will be tangential if only if  $(\bar{x}_2, \bar{y}_2) = (s \cdot \zeta_2, s \cdot \eta_2)$ . If the centre is to be included in  $D_0$  then  $s \in (-1, 1)$ .

Then the arc described by the probe is given by,

$$\bar{x}_2(T) = sr_0 \cos(\theta_1 + \tau) + (s - 1)r_0 \cos(T + \bar{\tau}), \quad (12)$$

$$\bar{y}_2(T) = sr_0 \sin(\theta_1 + \tau) + (s - 1)r_0 \sin(T + \bar{\tau}), \quad (13)$$

which depends on the time  $T \in [0, \theta_2]$ .

We want,

$$\bar{x}_2(\theta_2)^2 + \bar{y}_2(\theta_2)^2 = r_0^2(2s^2 + 2s - 1 + 2s(s - 1) \cos(\theta_1 - \theta_2 + \tau - \bar{\tau})) < r_0^2 \quad (14)$$

Let us consider  $f(s) = 2s(s - 1)(1 + \cos(\theta_1 - \theta_2 + \tau - \bar{\tau}))$ . Solving (14) is equivalent to finding  $s$  such that  $f(s) < 0$ . It is easy to see that  $f(s) < 0$  for  $s \in (0, 1)$  independent to the value of  $\theta_2$ .

Notice that if  $f(s)$  is minimal the distance to the origin is also minimal. It is easy to see that this is achieved when  $s = 1/2$ .

□

As before, let us define  $(\zeta_2^{(i)}, \eta_2^{(i)})$  as the change points, having for  $i$  odd change points from (10) to (11) and for  $i$  even change points from (11) to (10). As we have already said we will find a sequence of fixed points  $(\bar{x}_2^{(i)}, \bar{y}_2^{(i)})$  that make the trajectory tend to the origin.

**Lemma 4.3** *Let  $(\bar{x}_2^{(i)}, \bar{y}_2^{(i)})$  be the sequence of new fixed points for the control strategy and  $(\zeta_2^{(i)}, \eta_2^{(i)})$  the sequence of fixed points. If we choose  $\bar{x}_2^{(i)} = \zeta_2^{(2i+1)}/2$  and  $\bar{y}_2^{(i)} = \eta_2^{(2i+1)}/2$  then the sequence of change points  $(\zeta_2^{(i)}, \eta_2^{(i)})$  tend to the origin and so does the trajectory.*

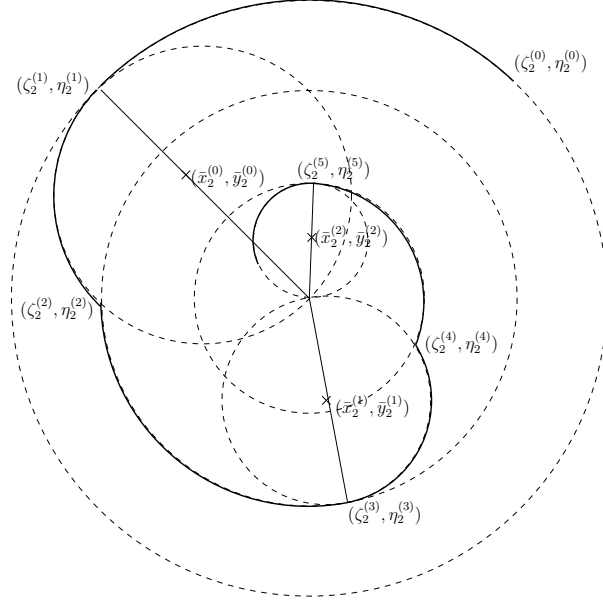


Figure 10: *Sequence of fixed points and the projection of the probe's trajectory in the centre plane.*

### Proof

Let us consider  $r^{(i)} = \sqrt{(\zeta^{(i)})^2 + (\eta^{(i)})^2}$ . It is easy to see that  $r^{2i} = r^{(2i+1)}$  as the change points  $(\zeta^{2i}, \eta^{2i})$  and  $(\zeta^{2i+1}, \eta^{2i+1})$  belong to the same arc centred on the origin.

As a consequence of lemma 4.2 we can see that taking  $(\bar{x}_2^{(i)}, \bar{y}_2^{(i)}) = (\zeta^{(2i+1)}/2, \eta^{(2i+1)}/2)$  we get,

$$r^{2i+1} > r^{2i+2}.$$

So we have that  $r^{2i} > r^{2i+2}$  and the sequence for change points tend to the origin and so does the projection of the trajectory. □

So taking the sequence of new fixed points  $(\bar{x}_2^{(i)}, \bar{y}_2^{(i)}) = (\zeta_2^{(2i+1)}/2, \eta_2^{(2i+1)}/2)$  the central movement will tend to the origin as can be seen in Figure 10.

## 4.2 Choosing the New Sail Orientation $(\alpha, \delta)$

In Sections 4.1.1 and 4.1.2 we have found an ideal sequence of fixed points to control the instability of  $p_0$ . As we have already said the fixed points live on a 2D surface parametrised by  $\alpha$  and  $\delta$  in a 6D phase space. So we might not be able to find a sail orientation  $\alpha_1$  and  $\delta_1$  so that the fixed point is one of the described before.

As we do not know explicitly the 2D surface of fixed points  $(p(\alpha, \delta))$ , in Section 3.1 we have seen how to find the linear approximation of this surface. So we would like to find  $h = (\alpha - \alpha_0, \delta - \delta_0)^T$  such that,

$$\bar{p} - p_0 = Dp \cdot h, \tag{15}$$

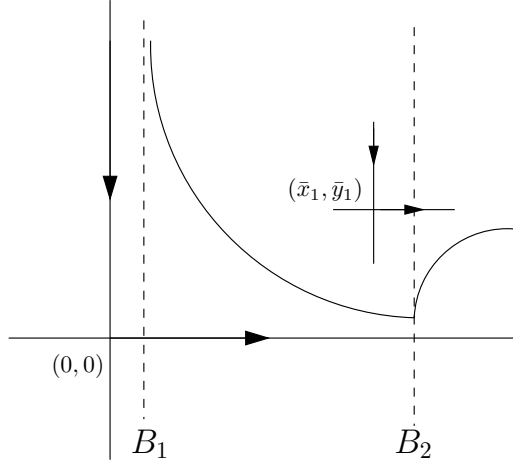


Figure 11: Possible position of the new fixed point  $p(\alpha_1, \delta_1)$  in the saddle projection that will not control the unstable behaviour.

where  $\bar{p}$  is the desired new fixed point (described in Section 4.1.1 and 4.1.2). Notice that (15) is (3) rewritten and that it has 6 equations and 2 unknowns. We would like to find  $\alpha_1, \delta_1$  such that  $\|\bar{p} - p(\alpha_1, \delta_1)\|$  is small enough.

Notice that although  $\|\bar{p} - p(\alpha_1, \delta_1)\|$  can be small  $p(\alpha_1, \delta_1)$  may not be able to control the instability due to the saddle part: If the projection of  $p(\alpha_1, \delta_1)$  on the saddle plane is on the left hand side of  $B_2$  then the unstable direction of  $p(\alpha_1, \delta_1)$  will not bring the probe back (see Figure 11). So we will fix one of the components of  $\bar{p}$ , having to find the fixed points in a 1D surface.

We will now give more details of the process described above. As said before, Sections 4.1.1 and 4.1.2 show the ideal position for the new fixed point ( $\bar{p}$ ). The coordinates of  $\bar{p}$  are given in the  $\{p_0; \vec{v}_1, \dots, \vec{v}_6\}$  reference system and equation (15) is in synodical coordinates. So we first have to change the base. Let  $M_v$  be the matrix that has  $\vec{v}_i$  for  $i = 1, \dots, 6$  as columns and  $s = (s_1, \dots, s_6)$  are the coordinates of the desired new fixed point ( $\bar{p}$ ) in this coordinate system. Then if  $A = M_v^{-1} Dp$  equation (15) becomes,

$$s^T = A \cdot h. \quad (16)$$

To avoid problems in the saddle behaviour we will fix  $s_1$ :

1. If  $a_{11} = a_{12} = 0 \iff \frac{\partial p}{\partial \alpha}, \frac{\partial p}{\partial \delta} \perp \vec{v}_1$ :

In this case there are no fixed points using the linear approximation for which its saddle behaviour brings the sail back.

2. If  $a_{11} = \max(|a_{11}|, |a_{12}|)$ :

$$s_1 = a_{11}h_1 + a_{12}h_2 \Rightarrow h_1 = \frac{s_1 - a_{12}h_2}{a_{11}}, \quad (17)$$

3. If  $a_{12} = \max(|a_{11}|, |a_{12}|)$ :

$$s_1 = a_{11}h_1 + a_{12}h_2 \Rightarrow h_2 = \frac{s_1 - a_{11}h_1}{a_{12}}, \quad (18)$$

This reduces (16) into  $\hat{s} = \hat{A} \cdot \hat{h}$  (5 equations and 1 unknown). Then  $\hat{h}$  so that  $\|\hat{s} - \hat{A} \cdot \hat{h}\|$  is minimal is,

$$\hat{h} = (\hat{A}^T \hat{A})^{-1} \hat{A}^T s. \quad (19)$$

### 4.3 Summary of the Control Algorithm

Suppose  $p_0$  is a fixed points for  $\alpha = \alpha_0, \delta = \delta_0$  that is linearly unstable. Let  $\{\lambda_i, \vec{v}_i\}_{i=1,\dots,6}$  be the eigenvalues and eigenvectors for  $D_X f(p_0)$ . We will fix a reference system  $\{p_0; \vec{v}_1, \dots, \vec{v}_6\}$  where,

- $p_0$  is the fixed point.
- $\vec{v}_1$  is the unstable eigenvector ( $+\lambda$ ).
- $\vec{v}_2$  is the stable eigenvector ( $-\lambda$ ).
- $\vec{v}_3, \vec{v}_4$  is the couple that defines one of the central movements ( $\pm i\omega_1$ ).
- $\vec{v}_5, \vec{v}_6$  defines the second central movement ( $\pm i\omega_2$ ).

From now on the trajectories will be seen in this reference system ( $x(t^*) = \sum s_i \vec{v}_i$ ), being  $(s_1, \dots, s_6)$  the coordinates of the trajectory in this reference system.

Let  $\varepsilon_{max}$  be the maximal distance we will allow to escape from the fixed point and  $\varepsilon_{min}$  the closest distance to the fixed point, needed when the probe is coming back (see Section 4.1.1). These constants depend on the mission objectives and the dynamical properties.

We start with the probe close to the fixed point  $p_0$  with  $\alpha = \alpha_0, \delta = \delta_0$ . When  $|s_1| > \varepsilon_{max}$ , the probe is far from  $p_0$ , we chose the appropriate  $\alpha_1, \delta_1$  that takes the probe back to a neighbourhood of  $p_0$  (see 4.2) and change the sail orientation ( $\alpha = \alpha_1, \delta = \delta_1$ ). When  $|s_1| < \varepsilon_{min}$ , the sail is close to  $p_0$  and we change the sail orientation back to  $\alpha = \alpha_0, \delta = \delta_0$ . This process is then restarted.

## 5 Mission Application

We have seen a technique that uses dynamical system tools and permits a solar sail maintain its trajectory close to a fixed point. This is something that cannot be done with a traditional satellite as a high amount of fuel is required. We would like to illustrate how this control technique behaves with missions that are now being developed as the Geostorm Warning and the Polar Observer Missions.

First we will briefly explain what the two missions consist and how to use the control techniques on them. Finally, several simulations have been done and we will explain the results obtained.

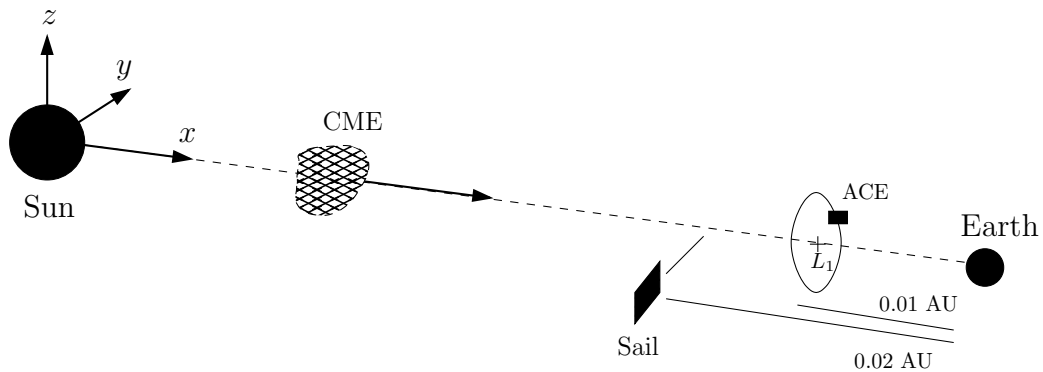


Figure 12: *Schematic representation of the position of the Geostorm Mission (not to scale).*

## 5.1 The Geostorm Mission

Its primary goal is to provide enhanced warning of geomagnetic storms to allow to take preventive actions to protect vulnerable systems. Geomagnetic storms are principally the result of Coronal Mass Ejections (CME), the violent release of large volumes of plasma from the solar corona. The impact of CME on the Earth's magnetosphere can change its magnetic field and produce electromagnetic storms.

Currently predictions of future activity are made by the National Oceanic Atmospheric Administration (NOAA) Space Environment Centre in Colorado using terrestrial data and real-time solar wind data obtained from the Advanced Compositions Explorer (ACE) spacecraft. The ACE spacecraft is stationed on a halo orbit near  $L_1$ , at about 0.01 AU from the Earth. From this position the spacecraft has continuous view of the Sun and communication with the Earth. Since the spacecraft is located sun wards of the Earth, the solar wind disturbances sensed by the instruments on board the ACE spacecraft are used to provide early warning of the impinging geomagnetic storms. Typically predictions of order 1 hour can be made from the  $L_1$  Lagrange point.

The enhanced storm warning provided by ACE is limited by the need to orbit the  $L_1$  point. However, since solar sails add an extra force to the dynamics of the orbit, the location of  $L_1$  can be artificially displaced, as has been shown in Section 3. The goal of Geostorm is to station a solar sail twice as far from the Earth than  $L_1$  while remaining close to the Earth-Sun line as can be seen in Figure 12. Since the CME will be detected earlier than by ACE the warning times and alerts will be at least doubled.

For this mission the solar sail is firstly transferred to a conventional halo orbit at  $L_1$ . At  $L_1$  the sail would be deployed and transferred to its location at 0.98 AU from the Sun. Once we arrive near to these region a control strategy must be designed in order to deal with the instability of this region.

Studies of this mission have been made by McInnes [9] [8], Chen-Wan [12] and Lisano [7]. McInnes [9] [8] makes a description of the mission concept, studies where the spacecraft should be placed and what sail could be used for this specific mission, but does not describe the trajectory that the sail should follow and what control techniques should be

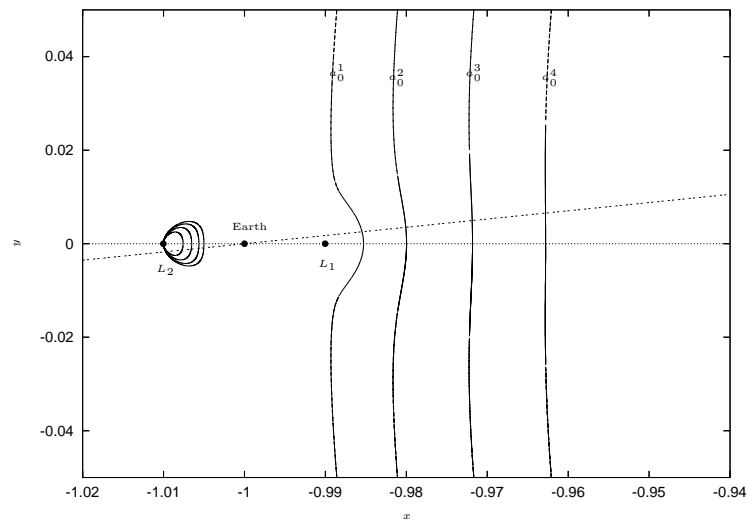


Figure 13: *Relation of the fixed point for different values of  $\beta$ , the read points correspond to linearly unstable points and in green the linearly stable fixed points. ( $a_0^1 = 0.17$ ,  $a_0^2 = 0.3$ ,  $a_0^3 = 0.46$  and  $a_0^4 = 0.61$ )*

used in order to control the instability of the trajectory. There we can see that a characteristic acceleration of  $a_0 = 0.3\text{mm/s}^2$  is required so that the spacecraft is placed at a double distance from the Earth-Sun  $L_1$  point.

Further studies of station keeping strategies have been made by Chen-Wan [12] and Lisano [7]. Chen-Wan presents two different station keeping strategies, the first considered a constant characteristic acceleration and changes the sail orientation after some period of time in order to return the sail to its original position. The second strategy uses constant variation of the sail orientation for the same aim. On the other hand, Lisano, makes a more detailed description of different strategies for the transfer from the  $L_1$  halo orbit to the Sub- $L_1$  region, and uses similar strategies as Chen-Wan for the station keeping.

### 5.1.1 Mission Orbit

As it has already been said we want to displace the spacecraft at a double distance from the Earth-Sun  $L_1$  point. For this purpose we need  $a_0 = 0.3\text{ mm/s}^2$  ([9], [12], [8]). In Figure 13 we have plotted the position of the equilibrium points for different sail orientations and sail acceleration close to the Earth - Sun line. As a constant communications with the Earth is needed we must displace the Sail approximately  $10^\circ$  from this line. In this region the fixed points are linearly unstable.

We have taken a reference system ( $\{p_0; \vec{v}_1, \dots, \vec{v}_6\}$ ) such that the  $p_0$  is a fixed point satisfying the requirements explained before for a fixed sail orientation  $\alpha_0, \delta_0$ . We have done 1000 simulations with different initial conditions chosen in a random way. The control strategy has been applied up to 30 years and we have measured for each one the time between manoeuvres, the variation of the sail orientation  $(\alpha, \delta)$  and the variation of

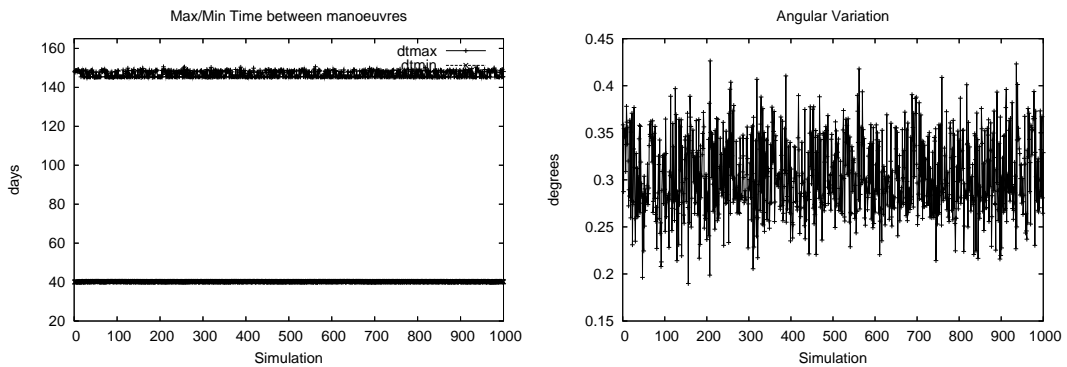


Figure 14: *Left: maximum and minimum time between manoeuvres vs number of simulation. Right: maximum angular variation between  $p_0$  and the probe trajectory vs number of simulation.*

the trajectory w.r.t  $p_0$ .

On the left hand side of Figure 14 we can see for each simulation the maximum and minimum time between manoeuvres. As we can see the minimum time between manoeuvres is around 40 days and the maximum time is around 146 days. On the right hand side of Figure 14 we have the maximum angular variation between the fixed point ( $p_0$ ) and the probe's trajectory seen from the Earth for each simulation. Notice that the maximum variation experienced is 0.45 degrees. The variation in the sail orientation is reflected in the variation of two angles  $\alpha$  and  $\delta$ . For these simulations we have seen that  $\alpha$  varies between 0.0695 and 0.0694 degrees every time the sail orientation is changed and  $\delta$  varies around 0.005 degrees.

Figure 15 shows the  $x, y$  and  $z$  oscillations with respect to time for 3 specific simulations. Notice that the  $x$  and  $y$  oscillate in a bounded region during all the time and  $z$  tends to zero. This illustrates the fact that, for this particular mission, the station keeping tends to take the probe's trajectory to the  $\{x, y\}$ - plane.

Finally in Figure 16 we can see one particular orbit after applying the control strategy on the  $\{x, y\}$ -plane (left), the  $\{x, z\}$ -plane (middle) and the 3D trajectory (left). Figure 17 shows the projection of this orbit on the saddle plane generated by the eigenvector  $\vec{v}_1, \vec{v}_2$  (left) and the projection on the other two central planes  $\vec{v}_3, \vec{v}_4$  (middle) and  $\vec{v}_5, \vec{v}_6$  (right).

## 5.2 The Polar Observer Mission

High latitude regions are of importance for a number of commercial and environmental interests. During the cold war the Arctic was a strategically important region, also the growing interest for the oil and mineral extraction of these regions may lead to a growing demand for communication services. The Arctic and Antarctic are also of great environmental importance and there is a requirement for relaying data from remote weather stations and automated monitoring platforms. Additional environmental requirements for polar services include continuous imaging of polar weather systems and monitoring of

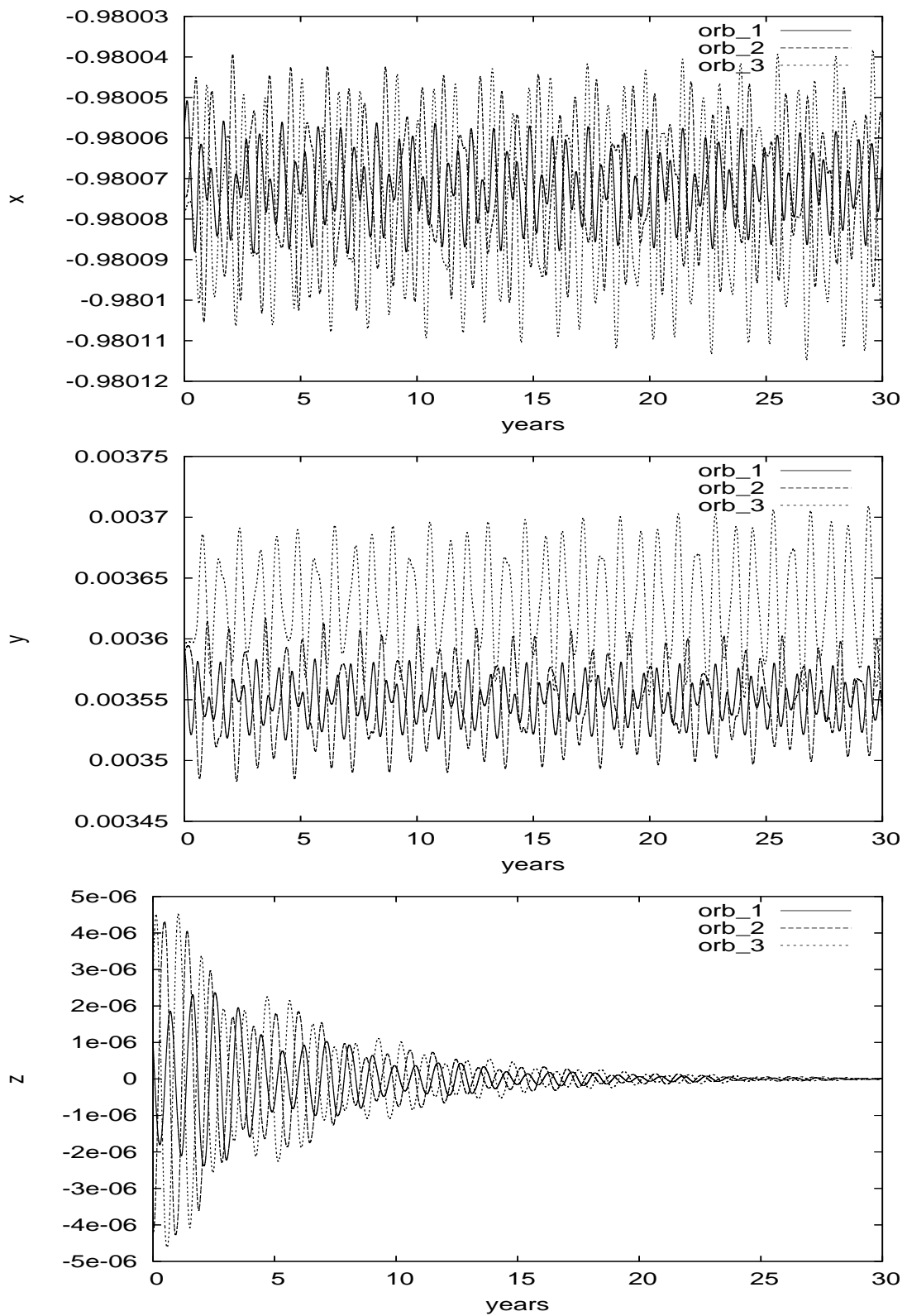


Figure 15: From left to right the variation of the probe's trajectory vs time on the  $x$ ,  $y$  and  $z$  direction.

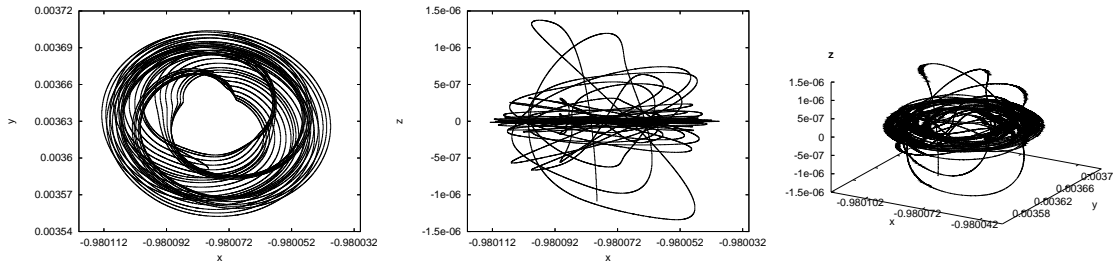


Figure 16: Trajectory followed by the probe for 30 years. Left:  $\{x, y\}$ - projection, Middle:  $\{x, z\}$ - projection, Right:  $\{x, y, z\}$ - projection

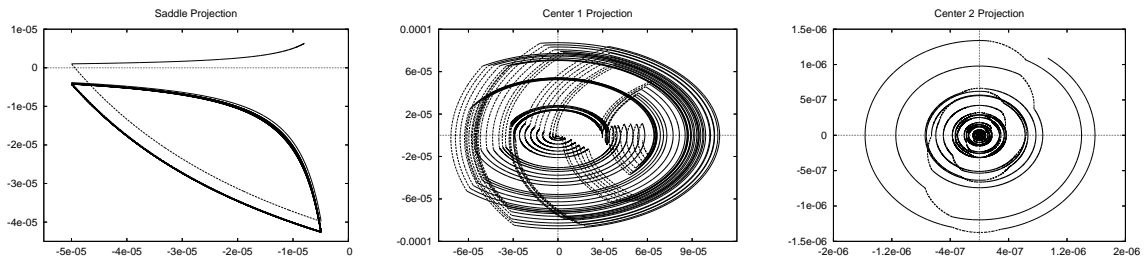


Figure 17: Trajectory followed by the probe for 30 years. Left: Projection of the trajectory on the saddle plane, Middle: Projection of the trajectory in one of the centre planes  $(\vec{v}_3, \vec{v}_4)$ , Right: Projection of the trajectory in the other centre planes  $(\vec{v}_5, \vec{v}_6)$ . In red the trajectory when the sail is set to  $\alpha_0, \delta_0$  and in green other orientations.

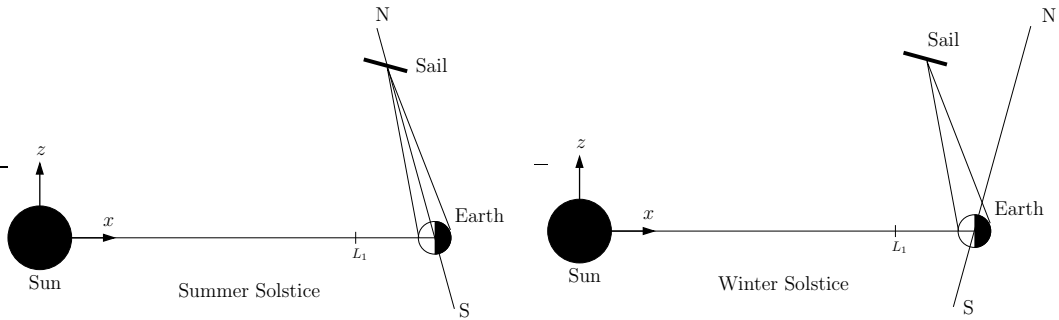


Figure 18: *Schematic representation of the Polar Observer Mission (not to scale).*

polar ice coverage for climate studies between others.

The limitation of geostationary orbits for such applications may be overcome to some extent using satellites in polar orbits. These orbits require the use of various satellites for a complete mapping or having to wait between imaging. Similarly communications services can be provided using high inclination Molniya orbits or through constellation satellites in low Earth orbits. While such systems are well suited for infrequent communications, they are too expensive for real-time relaying data.

As solar sails provide a wide range of new artificial equilibrium points, some of these equilibrium points can be used to place a sail to have constant viewing of the Polar regions of the Earth. As the Earth's inclination is of about  $23.4^\circ$  we must place the solar sail at  $66.6^\circ$  from the ecliptic plane. Notice that as the Earth orbits around the Sun, the sail will maintain its fixed position with respect to the Earth but it will not always have the same view at the pole due to the Earth's inclination, see Figure 18. Having the sail perfectly situated on the north pole during the summer solstice, and during the winter solstice the sail will appear displaced over the horizon, having still some imaging of the north pole.

More information about the Polar Observer can be found in [9] and [8], where a more detailed background of the mission is described as well as the choice of the mission orbit and sail. This mission has not been as studied as the Geostorm mission probably due to the fact that the sail must be displaced at about 3.9 million km from the Earth, having then low resolution imaging of the Poles.

### 5.2.1 Mission Orbit

Notice that as the sail performance increases the equilibrium points come closer to the Earth. But as a first mission we are dealing with small resolution sails. In Figure 19 we can see the relation between the sail effectiveness and the equilibrium point. We will take  $a_0 = 0.46\text{mm/s}^2$  as it is the minimum sail characteristic acceleration that makes the solar sail be placed over the north pole. In these regions the points are also linearly unstable.

As before we have also taken a reference system  $\{p_0; \vec{v}_1, \dots, \vec{v}_6\}$  so that the fixed point  $p_0$  satisfies the required conditions for a fixed sail orientation  $\alpha_0, \delta_0$ . We have also done 1000 simulations applying the control strategy up to 30 years with random initial conditions and measured the time between manoeuvres, the variation of the sail

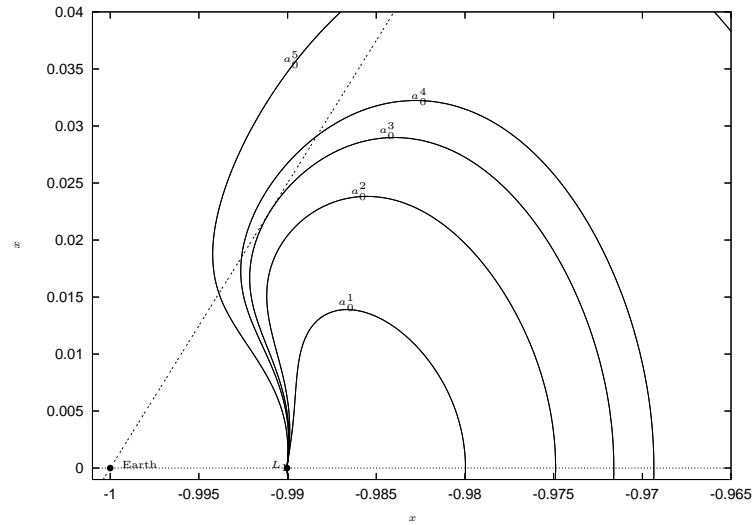


Figure 19: Relation of the fixed point for different values of  $\beta$ . ( $a_0^1 = 0.3$ ,  $a_0^2 = 0.4$ ,  $a_0^3 = 0.46$ ,  $a_0^4 = 0.5$  and  $a_0^5 = 0.7$ )

orientation and the angular variation w.r.t  $p_0$ .

In the left hand side of Figure 20 we can see for each simulation the maximum and minimum time between manoeuvres. Now the minimum time between manoeuvres is always around 59 days and the maximum time is around 187 days. In the right hand side of Figure 20 we have the maximum angular variation between the fixed point ( $p_0$ ) and the probe's trajectory for each simulation, where the maximum variation experienced is around 0.3 degrees. In these simulations we have seen that  $\alpha$  varies between 0.03 and 0.02 degrees every time the sail orientation is changed and  $\delta$  varies around 0.02 degrees.

Figure 23 shows the  $x, y$  and  $z$  oscillations with respect to time for 3 specific simulations. Now the trajectories oscillate in the three directions but all of them in a bounded region. In Figure 21 we can see the one particular orbit after applying the control strategy on the  $\{x, y\}$ -plane (left), the  $\{x, z\}$ -plane (middle) and the 3D trajectory (left). We can see how on the  $\{x, z\}$ - projection the sail seems to follow a quasi-periodic motion.

Finally in Figure 22 shows the projection of this orbit on the saddle plane generated by the eigenvector  $\vec{v}_1, \vec{v}_2$  (left) and the projection on the other two central planes  $\vec{v}_3, \vec{v}_4$  (middle) and  $\vec{v}_5, \vec{v}_6$  (right).

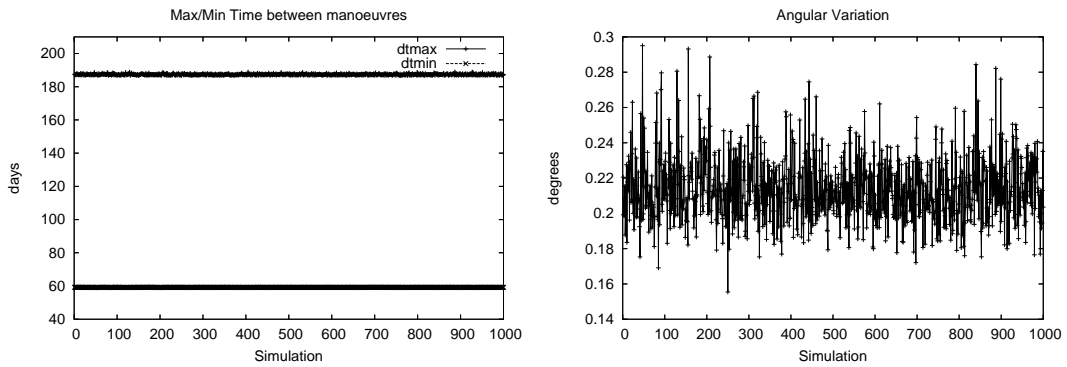


Figure 20: *Left: maximum and minimum time between manoeuvres vs number of simulation. Right: maximum angular variation between  $p_0$  and the probe trajectory vs number of simulation.*

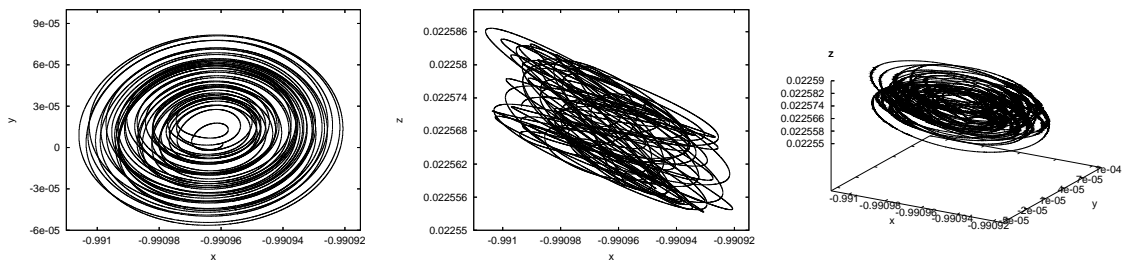


Figure 21: *Trajectory followed by the probe for 30 years. Left:  $\{x, y\}$ - projection, Middle:  $\{x, z\}$ - projection, Right:  $\{x, y, z\}$ - projection*

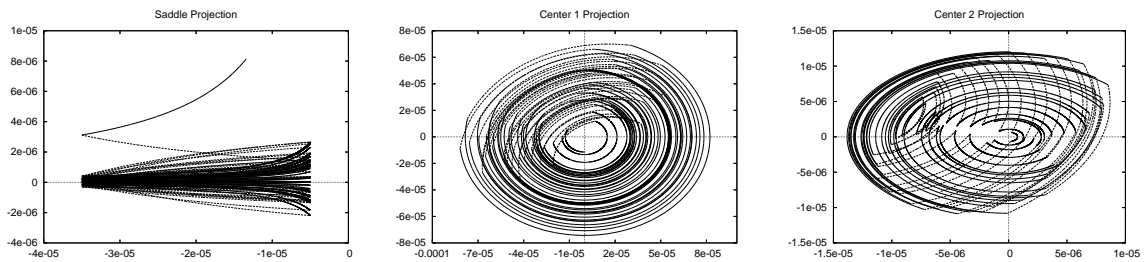


Figure 22: *Trajectory followed by the probe for 30 years. Left: Projection of the trajectory on the saddle plane, Middle: Projection of the trajectory in one of the centre planes  $(\vec{v}_3, \vec{v}_4)$ , Right: Projection of the trajectory in the other centre planes  $(\vec{v}_5, \vec{v}_6)$ . In red the trajectory when the sail is set to  $\alpha_0, \delta_0$  and in green other orientations.*

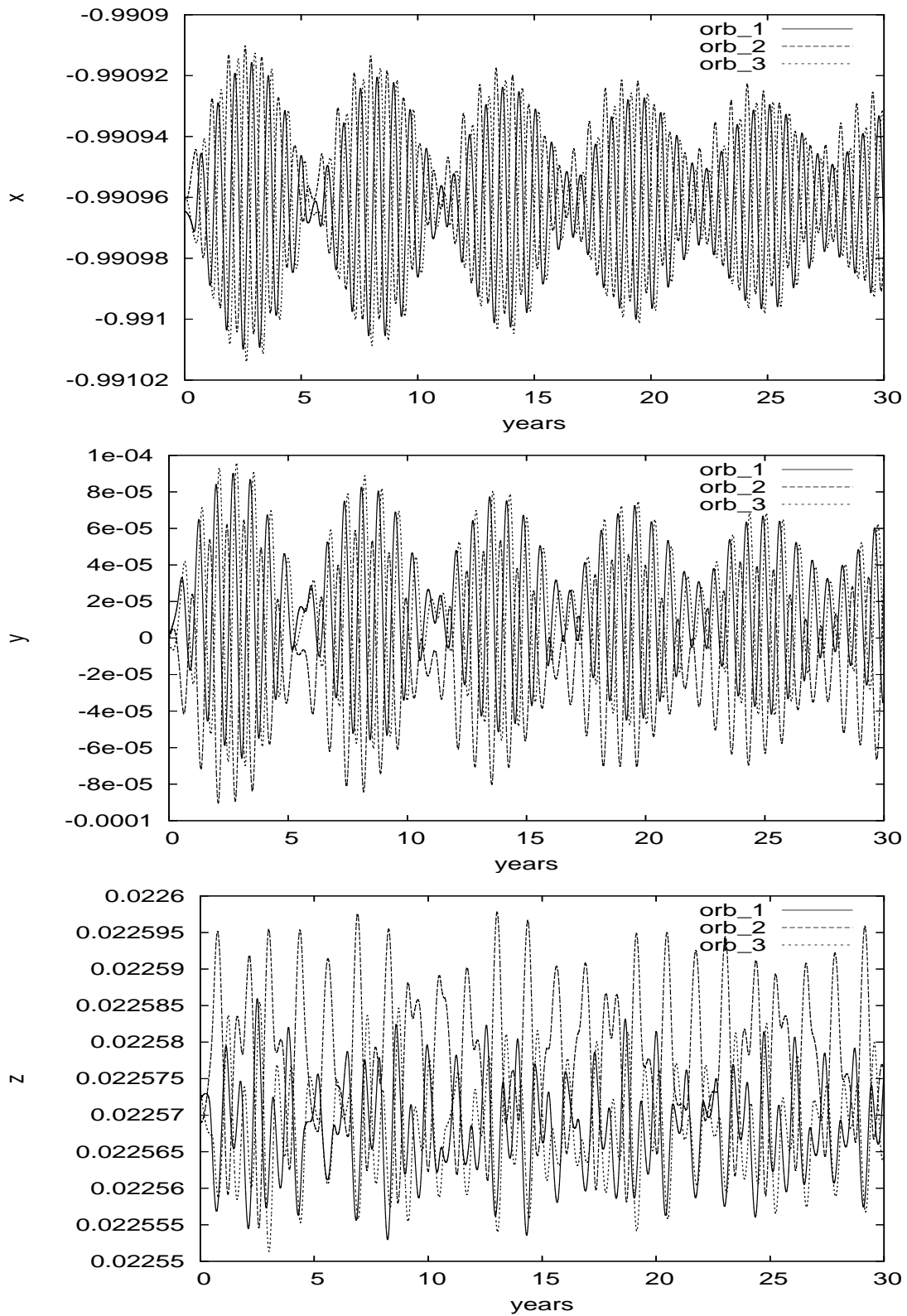


Figure 23: From left to right the variation of the probe's trajectory vs time on the  $x$ ,  $y$  and  $z$  direction.

## 6 Sensitivity to Errors During the Control Strategy

It is a known fact that during a mission the position and velocity of the probe will not be determined exactly, this has an effect on the decisions taken by the control algorithm. Errors on the sail orientation will also be made and have an important effect in the probe's trajectory. We will see the effect of these errors in our control strategy.

Let us first consider the errors on the position and velocity of the probe. As we have seen in previous sections the sail orientation will be changed when the probe is at a certain distance of the fixed point in the saddle plane projection. Each time the algorithm asks itself if the sail orientation has to be changed, the probe's position in the phase space has some small error. If the sail orientation is changed the new fixed point will be found using the wrong position of the probe. So errors made on the measurement of the probe's position will make the algorithm take decision of changing the sail orientation when not desired and the new fixed points position will also be modified. If this errors are not very big the difference between changing the sail orientation a little before or after in time will not affect the control of the probe.

We have supposed that all the errors follow a normal distribution with mean 0. We have taken a precision of the space slant of  $\approx 1\text{m}$  and  $\approx 2 - 3\text{milli-arc-seconds}$  in the angle determination. The precision in speed is around  $20 - 30\text{micro/seconds}$ . These errors magnitudes reflect as errors of order  $10^{-8}$  in the saddle plane projection, these effect is almost neglected.

We have done 1000 simulation taking the same initial conditions as in Sections 5.1.1 and 5.2.1 adding the uncertainty in the position and velocity measurement. We have seen that the results obtained are similar, for all the 1000 simulations in both missions the probe's trajectory does not escape after 30 years. The average time between manoeuvre's is slightly changed and so are the angular variation in the trajectories position with respect to the initial fixed point (see Table 1 and 2).

Lets now consider the errors due to the sail orientation. As we will now see these errors have a more important effect on the sail trajectory and the controllability of the probe. Each time the sail orientation is changed an error in its orientation is made ( $\alpha = \alpha_1 + \epsilon_\alpha$ ,  $\delta = \delta_1 + \epsilon_\delta$ ). Then the new fixed point  $p_1$  is shifted  $p(\alpha, \delta) = p(\alpha_1, \delta_1) + \epsilon_p$  and so do the stable and unstable directions  $\vec{v}_{1,2}(\alpha, \delta) = \vec{v}_{1,2}(\alpha_1, \delta_1) + \epsilon_v$ . These variations can make the probe's trajectory not to come close to  $p_0$ , as  $p(\alpha, \delta)$  can be placed on the incorrect side of the saddle (see Section 4.2) or the the central behaviour can blow up.

Depending on the nature of the region where the fixed point is placed the control strategy will be able to deal with bigger errors in the sail orientation. It will all depend on the variation of the fixed point and the eigenvectors with respect to the sail orientation.

We have also done 1000 simulations taking the same initial conditions as in Sections 5.1.1 and 5.2.1 and introducing the uncertainties on sail orientation and probe's position and velocity.

Tables 1 and 2 show the results of all these simulations for the Geostorm and Polar Observer missions respectively. On the first line we have the results for the simulations when no errors are taken into account. On the second line there are the results when only error on the position and velocity determination are made. Finally the third line contains

	% Success	Max. Time	Min. Time	Ang. Vari.
No Error	100%	146.77 days	40.20 days	$0.3^\circ$
Error Pos.	100%	146.82 days	40.19 days	$0.3^\circ$
Error Pos. + Orient.	100%	376.78 days	32.60 days	$1.2^\circ$

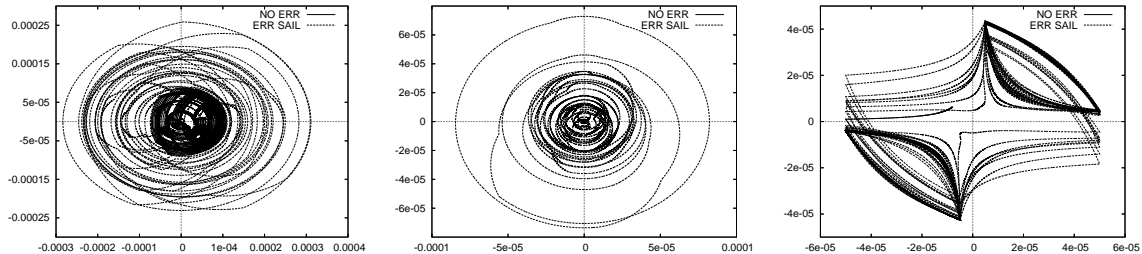
Table 1: *Statistics for the Geostorm mission 1000 simulations.*

Figure 24: *Geostorm: In red the trajectory followed by the probe when no error during the control algorithm are made. In green the trajectory followed by the probe when errors on the position and sail orientation are made. From left to right the projection of the sail's trajectory on the saddle, centre 1 and centre 2 planes.*

the results when all the errors are taken into account (sail orientation and position + velocity determination). Notice that Table 2 has a fourth line, this is because for the Polar Observer we have done simulations with errors on the sail orientation of order  $0.01^\circ$  and  $0.001^\circ$  while for the Geostorm the errors made on the sail orientation are only of order  $0.01^\circ$ . Column 2 shows the % of simulations that succeed in controlling the probe, column 3 and 4 have the average maximum and minimum time between manoeuvres respectively and column 5 has the average angular variation of the trajectory as seen from the Earth.

If we look at Table 1 we can see that for the Geostorm mission all of the 1000 simulations succeed even if errors on the sail orientation or on the determination of the probe's position and velocity are made. As we can see there is practically no change between including or not the error in the position determination, but it does change if we introduce errors on the sail orientation. This is due to the big variation in the fixed points position when these last errors are taken into account. As we can see the angular variation between is almost doubled when all the errors are taken into account, this is because now the probe's trajectory moves on both sides of the saddle as can be seen in Figure 24. In this figure we can see the difference between the trajectory followed by the probe when errors in the sail orientation are added for the Geostorm.

In Table 2 we have the results for 1000 simulations for the Polar Observer. As the table shows, our control strategy, in this particular mission is not able to deal with errors on the sail orientation of order  $0.01^\circ$ . As we have seen in Table 1, this magnitude of errors were acceptable in the Geostorm, this is due to the nature of the region: we recall that in Section 5.2.1 we have seen that the variation of the sail orientation is  $\alpha \approx 0.03^\circ$

	% Success	Max. Time	Min. Time	Ang. Vari.
No Error	100%	187.36 days	59.16 days	$0.21^\circ$
Error Pos.	100%	187.86 days	58.89 days	$0.21^\circ$
Error Pos. + Orient. *	33.9%	490.5 days	41.16 days	$0.56^\circ$
Error Pos. + Orient. †	100%	246.85 days	55.08 days	$0.36^\circ$

Table 2: Statistics for the Polar Observer mission 1000 simulations. For \* we have take error on the sail orientation of order  $0.01^\circ$  and for † the errors on the sail orientation of order  $0.001^\circ$ .

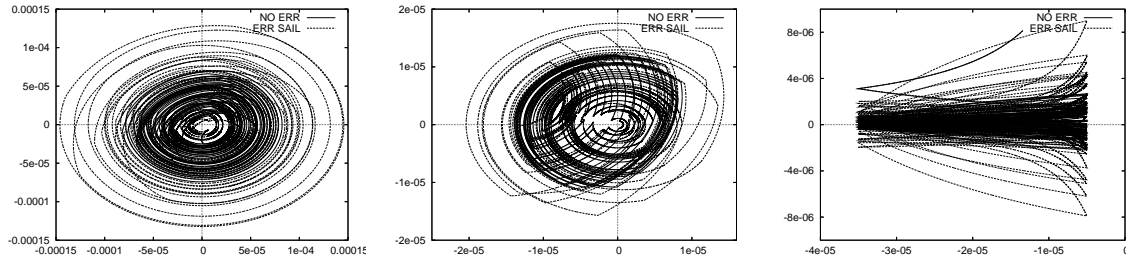


Figure 25: Polar Observer: In red the trajectory followed by the probe when no error during the control algorithm are made. In green the trajectory followed by the probe when errors on the position and sail orientation are made. From left to right the projection of the sail's trajectory on the saddle, centre 1 and centre 2 planes.

and  $\delta \approx 0.01^\circ$ . This is way we need more precision on the sail orientation to be able to control the probe.

As it happened on the Geostorm mission we can see that the time between manoeuvres practically does not change when the errors on the position determination are included, and the same happens for the angular variation. But it does change when errors on the sail orientation are introduced.

In Figure 25 we can see two different trajectories for the same initial condition, one made with no errors on the control strategy and the other with errors during the control strategy for the Polar Observer.

We must also mention that there is a big relation between the variation on the sail orientation ( $\Delta\alpha, \Delta\delta$ ) and the two bound that define the region of movement on the saddle projection ( $B_1 = \{x_1 = \varepsilon_{min}\}$  and  $B_2 = \{x_1 = \varepsilon_{max}\}$ ). Let  $\Delta\varepsilon = \varepsilon_{max} - \varepsilon_{min}$ , then as  $\Delta\varepsilon$  gets bigger the variation in the sail orientation is bigger. Although  $\Delta\varepsilon$  cannot be too big, because we would have problems in the station keeping algorithm. Notice that  $\varepsilon_{max}$  must be inside the limits where the linear behaviour is valid to define the behaviour of the probe, which is strictly related with the nature of the fixed point and its vicinity.

## 7 Conclusions

In this paper we present a new way of controlling a solar sail close to an unstable fixed point by using dynamical system tools. We have studied the natural dynamics of the system close to a fixed point and the variation of this point when the sail orientation ( $\alpha$ ,  $\delta$ ) is changed. This knowledge has permitted us design a control strategy that maintains a probe's trajectory close to an unstable equilibrium.

We have tested this strategy with two different missions, the 'Geostorm Warning Mission' and the 'Polar Observer'. In both cases the probe managed to stay close to the fixed point for 30 years. We have also tested the controllability of the algorithm including errors in the prediction of the probe's position and velocity and errors in the sail orientation angles ( $\alpha$ ,  $\delta$ ). We have seen that the errors on the position and velocity do not produce important changes in the sail's trajectory and its controllability. The errors on the sail's orientation are more relevant and give more variations on the trajectory followed by the probe.

As we have seen, the controllability of the sail is strictly related with the nature of the neighbourhood of the fixed point where we want to maintain the sail. If the variations of the fixed points and the eigendirections is understood, we can be understand the dynamics and, therefore, the reasons that make the control more or less difficult. As we have seen in the Polar Observer Mission, more precision on the sail orientation was required to be able to control the probe.

Finally let us mention that the strategy proposed here does not require previous planning, the decisions taken by the probe depend only on its position on the phase space, that is known at each moment. In this way, you do not have to plan the control strategy in advance and errors made during the manoeuvres can be rectified easily.

## 8 Acknowledgements

This work has been supported by the MEC grant MTM2006-11265 and the CIRIT grant 2005SGR01028. We thank G. Vulpetti for his comments on the position and attitude errors, and G. Gómez for his remarks and several discussions.

## References

- [1] J. Bookless and C. R. McInnes. Control of lagrange point orbits using solar sail propulsion. In *56th International Astronautical Congress*, 2005.
- [2] A. Farrés and A. Jorba. Solar sail surfing along families of equilibrium points. In *58th International Astronautical Congress*, Hyderabad, India, September 2007.
- [3] A. Farrés and A. Jorba. Station keeping close to unstable equilibrium points with a solar sail. In *AAS/AIAA Astrodynamics Specialist Conference*, Mackinac Island, Michigan, August 2007.

- [4] G. Gómez, J. Llibre, R. Martínez, and C. Simó. Station keeping of libration point orbits. ESOC contract 5648/83/D/JS(SC), final report, European Space Agency, 1985.
- [5] G. Gómez, J. Llibre, R. Martínez, and C. Simó. *Dynamics and mission design near libration points. Vol. I*, volume 2 of *World Scientific Monograph Series in Mathematics*. World Scientific Publishing Co. Inc., River Edge, NJ, 2001.
- [6] D. Lawrence and S. Piggott. Solar sailing trajectory control for sub-11 stationkeeping. *AIAA 2004-5014*, 2004.
- [7] M. Lisano. Solar sail transfer trajectory design and station keeping control for missions to sub-11 equilibrium region. In *15th AAS/AIAA Space Flight Mechanics Conference*, Colorado, January 2005. AAS 05-219.
- [8] M. Macdonald and C. R. McInnes. A near - term road map for solar sailing. In *55th International Astronautical Congress*, Vancouver, Canada, 2004.
- [9] C. R. McInnes. *Solar Sailing: Technology, Dynamics and Mission Applications*. Springer-Praxis, 1999.
- [10] L. Rios-Reyes and D. Scheeres. Robust solar sail trajectory control for large pre-launch modelling errors. In *2005 AIAA Guidance, Navigation and Control Conference*, August 2005. AIAA-2005-6173.
- [11] V. Szebehely. *Theory of orbits, The restricted problem of three bodies*. Academic Press, 1967.
- [12] C.-W. L. Yen. Solar sail geostorm warning mission design. In *14th AAS/AIAA Space Flight Mechanics Conference*, Hawaii, February 2004. AAS 04-107.